Title

Allocation of gene products to daughter cells is determined by the age of the mother in single Escherichia coli cells

Journal

Proceedings of the Royal Society B, 287(1926)

ISSN

0962-8452

Authors

Shi, Chao

Chao, Lin

Proenca, Audrey Menegaz

et al.

Publication Date

2020-05-13

DOI

10.1098/rspb.2020.0569

Peer reviewed

PROCEEDINGS B

royalsocietypublishing.org/journal/rspb

Research

Cite this article: Shi C, Chao L, Proenca AM, Qiu A, Chao J, Rang CU. 2020 Allocation of gene products to daughter cells is determined by the age of the mother in single *Escherichia coli* cells. *Proc. R. Soc. B* **287**: 20200569.
http://dx.doi.org/10.1098/rspb.2020.0569

Received: 12 March 2020
Accepted: 14 April 2020

Subject Category:
Evolution

Subject Areas:
microbiology, evolution, computational biology

Keywords:
aging, bacterial aging, stochasticity, deterministic protein allocation, asymmetrical protein allocation

Author for correspondence:
Camilla U. Rang
e-mail: urang@ucsd.edu

†These authors contributed equally to this study.

Electronic supplementary material is available online at https://doi.org/10.6084/m9.figshare.c.4949670.

THE ROYAL SOCIETY PUBLISHING

Allocation of gene products to daughter cells is determined by the age of the mother in single *Escherichia coli* cells

Chao Shi[1,†], Lin Chao[1,†], Audrey Menegaz Proenca[1,2], Andrew Qiu[1], Jasper Chao[1] and Camilla U. Rang[1]

[1]Section of Ecology, Behavior and Evolution, Division of Biological Sciences, University of California San Diego, La Jolla, CA 92093-0116, USA
[2]Geobiology Laboratory, Institute of Petroleum and Natural Resources, Pontifícia Universidade Católica do Rio Grande do Sul, Porto Alegre, Brazil

CUR, 0000-0002-3589-7327

Gene expression and growth rate are highly stochastic in *Escherichia coli*. Some of the growth rate variations result from the deterministic and asymmetric partitioning of damage by the mother to its daughters. One daughter, denoted the old daughter, receives more damage, grows more slowly and ages. To determine if expressed gene products are also allocated asymmetrically, we compared the levels of expressed green fluorescence protein in growing daughters descending from the same mother. Our results show that old daughters were less fluorescent than new daughters. Moreover, old mothers, which were born as old daughters, produced daughters that were more asymmetric when compared to new mothers. Thus, variation in gene products in a clonal *E. coli* population also has a deterministic component. Because fluorescence levels and growth rates were positively correlated, the aging of old daughters appears to result from both the presence of both more damage and fewer expressed gene products.

1. Introduction

Gene expression and protein levels in individual cells are highly variable in clonal populations [1–10]. Because many gene-regulating elements have low copy numbers [11], the variation is attributed to stochastic sampling. For example, if the elements are Poisson distributed, they will have a mean of μ and a variance of σ^2, where $\mu = \sigma^2$, but the coefficient of variation for the relative difference between cells is $\sigma/\mu = 1/\sqrt{\mu}$, which increases with decreasing values of μ. Given that the amount of expressed gene products is an important component of cellular function and fitness, the amount of stochasticity is at first glance puzzling. A possible explanation is that cellular metabolism constrains the total pool of gene products and some genes are limited to a smaller, and perhaps suboptimal, number of regulatory elements. An additional explanation is that the variation is a form of bet hedging [12,13]. If the environment is changing or variable, a variant cell could have by chance the gene product level that is appropriate for that instance. Alternatively, the apparent stochasticity could result from yet uncovered deterministic causes [14–16].

Recent results have shown that the growth rate of single and clonal bacterial cells is also highly stochastic [17–19]. However, the growth rates were found to have a significant deterministic component that is controlled by the asymmetrical partitioning of non-genetic damage, such as oxidized or mistranslated proteins, by a mother bacterium to its two daughters. The allocation of more damage to one daughter by a mother bacterium is associated with the age of the maternal cell poles. Because a rod-shaped bacterium such as *Escherichia coli* divides at the midplane of its long axis, the poles formed at the midplane are new while the distal poles are older (figure 1). As a result, all *E. coli* cells have an old and a new pole. When a mother cell divides, one of its daughters receives the maternal

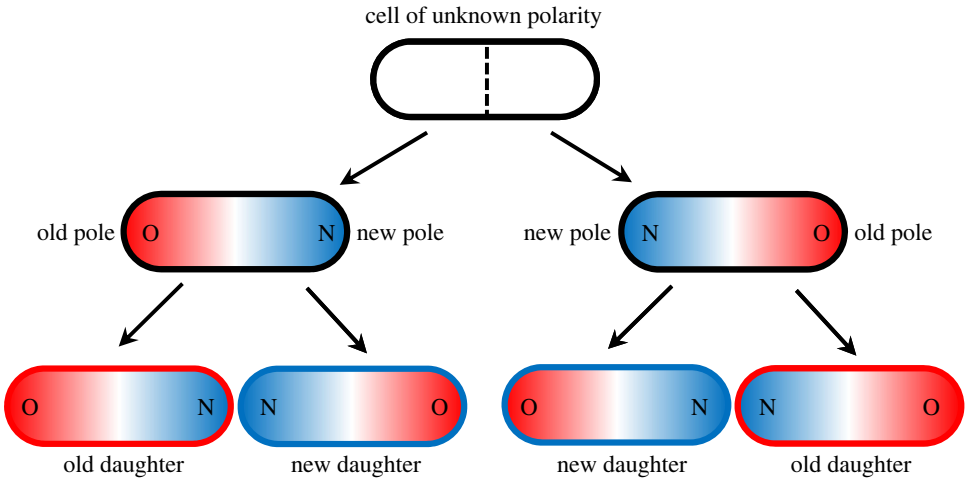

Figure 1. Assignment of old (red) and new (blue) poles and daughters in *E. coli*. Vertical, dotted line shows the middle and axial plane of the cell. Because the division plane cuts *E. coli* at the midpoint of the long axis, the poles formed at the division point are new and the distal poles are old. Note that if the polarity of the first cell is unknown, two divisions are required to determine old and new daughter. The outlines of the bottom four daughters in the figure are coloured red and blue to identify them as old and new daughters, while the intracellular red and blue colours identify the old and new poles, also designated as O and N. (Online version in colour.)

old pole and the other the new pole. The daughters are denoted, respectively, the old and new daughters. The evidence for the asymmetrical partitioning of damage is manifold. Old daughters have been shown to have a slower growth rate than new daughters [17,20–26]. The old pole and old daughters are more likely to harbour aggregates of damaged and synthetically misfolded proteins, and aggregate size is negatively correlated with cell growth rate [25,27]. If *dnaK*, the gene responsible to dismantling aggregates for repair, is knocked out in *E. coli* lineages of new daughters survive while lineages of old daughters perish [18]. Although early investigations reported that damage rates in standard laboratory culture were too low to generate an asymmetry between old and new daughters [23,28], follow-up studies have shown that a difference is detectable with improved microscopy and larger sample sizes [17,18,26].

The difference between growth rate of old and new daughters increases the variation between single cells. However, because the asymmetry is a deterministic component of bacterial cell division, the growth rate variation observed in a bacterial population, even in a clonal one, cannot be explained entirely by stochasticity. Because cell growth rates and ribosome number are positively correlated [29], it follows that the levels of expressed gene products could also be similarly correlated. We therefore investigated whether the levels of expressed proteins could also be asymmetrically distributed between old and new daughters. Previous studies of the stochasticity of expressed proteins in single cells did not look for possible differences between old and new daughters and pooled them as independent replicates. We found that new daughters overall contained higher levels of expressed proteins than old daughters. The difference between a pair of old and new daughters was greatest when the mother was born as an old daughter. Because old daughters have more damage, their lower level of expressed proteins could be explained by a competition model in which damage and proteins compete for space. Moreover, the level of expressed proteins correlated positively with the growth rate of the cells. From an evolutionary perspective, a growth rate difference between old and new daughters is beneficial because the resulting variation increases the efficiency of selection [24]. Thus, the variation in growth rates and expressed gene products in a clonal population of *E. coli* has a deterministic component that is evolutionarily advantageous.

2. Results

A constitutively expressed green fluorescent protein (GFP) was used as a proxy for the level of expressed proteins within and between individual single *E. coli* cells. The *gfp* mutant *mut3b* was purposely chosen as a rapid reporter because of its short maturation time and high diffusion rate [30,31] relative to the size and doubling times of the bacteria in our study (see Discussion). The size of GFP (238 amino acids) [32] is on the same order of magnitude as the mean protein size in *E. coli* (360 amino acids) [33]. Following protocols in Material and Methods, we generated time-lapse images of dividing cells and measured their elongation rates and fluorescence intensities. To ensure that the fluorescence images were not biased, care was taken to record within the dynamic range (below saturation) of the camera. Additionally, to correct for the diffractional scatter of fluorescence from a cell to its neighbours within a colony, all images were corrected by deconvolution. Sample sizes and statistical tests are provided in the figure legends.

(a) Protein levels are biased towards new poles and asymmetrical between old and new daughters

To investigate whether variation in expressed protein levels between *E. coli* cells has a deterministic component, we first analysed the GFP levels of micro-colonies of 1–4 cells and compared old and new daughter pairs descending from the same mother (hereafter old and new daughters; figure 1) shortly after division. Despite fluorescence levels varying considerably between cells (consistent with earlier studies [2,4,6]), we noted less fluorescence in old poles than the new poles rendering old daughters overall dimmer as we followed single cells dividing into two and four cells (figure 2*a*). To explore this further, we plotted the fluorescent profile of new and old daughters along the cells and normalized the daughters into

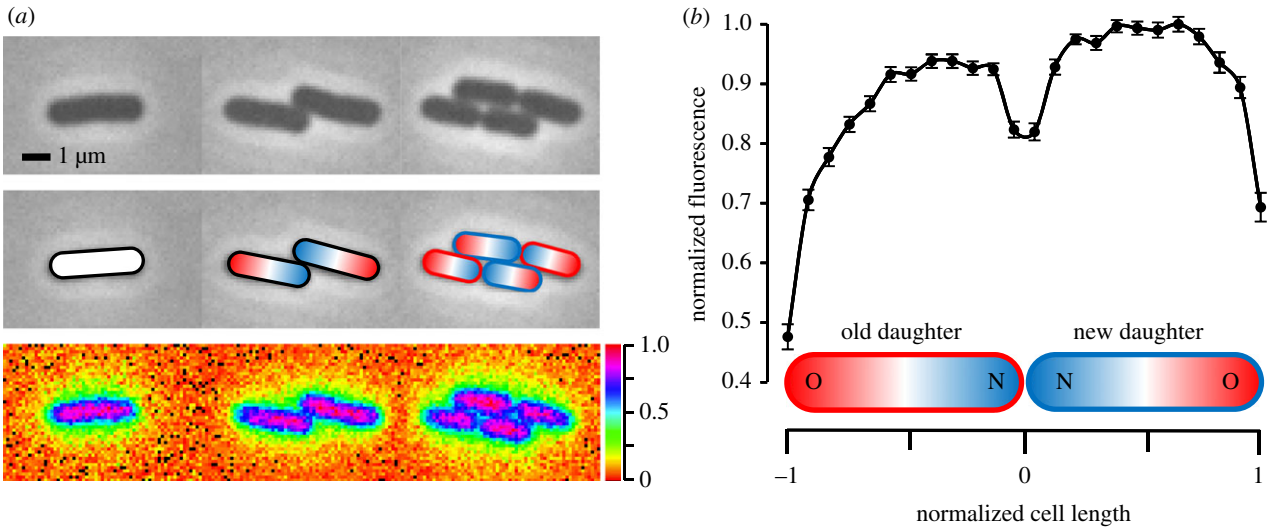

Figure 2. Intracellular fluorescent difference of single cells. (*a*) Time-lapse images of an *E. coli* bacterium dividing into two and four cells. Top row: Phase contrast. Middle row: Assignment of old (red) and new (blue) poles from the top row cells. Bottom row: Heat-map of fluorescent images of the top row cells, showing lesser intensity by the old poles (blue colour spots) than the new poles and inside the cells (pink colour). Scale on the right goes from highest intensity = pink, to lowest = orange. (*b*) Fluorescence profile along the cells of new and old daughter pairs with colour designation as in figure 1 for old (red) and new (blue) poles and daughters. The length of the cells is normalized for comparison ($n = 40$ pairs). Error bars show standard error of the mean (s.e.m.). (Online version in colour.)

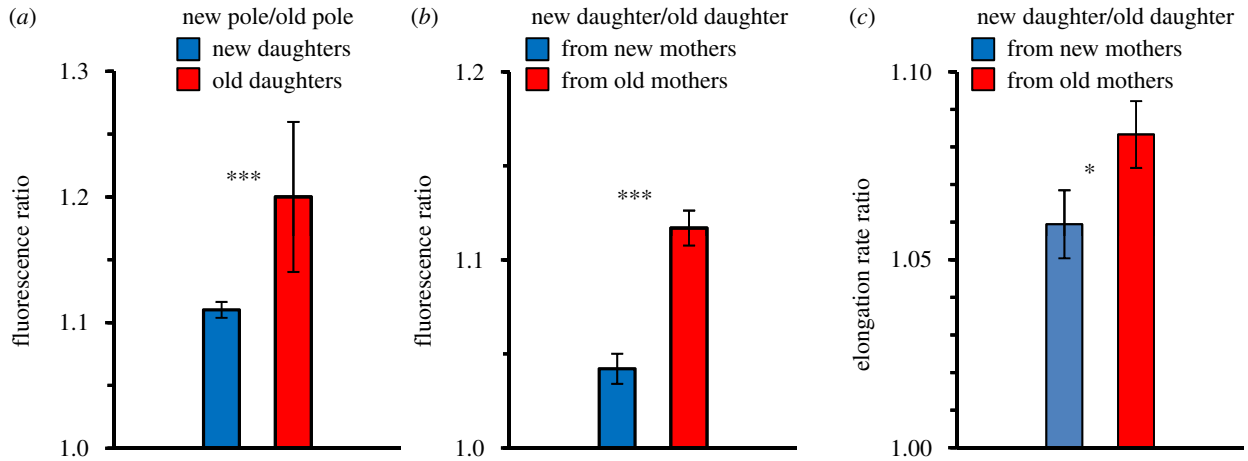

Figure 3. Ratios of fluorescence and elongation rates within and between cells. (*a*) Fluorescence ratio (new/old) of the two polar halves from old (red) and new (blue) daughters ($n = 404$ pairs). Old daughters show a higher asymmetry between the two polar halves than do new daughters. The ratio of fluorescence from the cell half that contains the oldest pole is 1.2 ± 0.06 ($p = 2.58 \times 10^{-97}$, two-tailed paired *t*-test) in favour of the half that contains the newest pole in old daughters, and 1.1 ± 0.006 ($p = 3.41 \times 10^{-48}$, two-tailed paired *t*-test) in new daughters. The difference between the two ratios was significant ($p = 2.8 \times 10^{-19}$, two-tailed non-paired *t*-test). New daughters in general had a higher fluorescence than old daughters with a ratio of 1.08 ± 0.004 ($p = 2.57 \times 10^{-65}$, two-tailed paired *t*-test). (*b*) Fluorescence ratio (new/old) of daughters from old (red) and new (blue) mothers. The ratio from old mothers was 1.12 ± 0.009 ($p = 1.68 \times 10^{-21}$, two-tailed paired *t*-test, $n = 178$ pairs) and from new mothers 1.04 ± 0.008 ($p = 1.78 \times 10^{-5}$, two-tailed paired *t*-test, $n = 177$ pairs). The difference between the two ratios was significant ($p = 2.75 \times 10^{-9}$, two-tailed non-paired *t*-test). Consistent with the same finding mentioned in figure 3*a*, new daughters in general had a higher fluorescence than old daughters with an average ratio of 1.08 ± 0.006 ($p = 4.67 \times 10^{-23}$, two-tailed paired *t*-test). (*c*) Ratio of elongation rate (see Material and Methods for details) of new over old daughters from new (blue) and old (red) mothers. The ratio from old mothers was 1.0833 ± 0.009 ($p = 1.12 \times 10^{-16}$, two-tailed paired *t*-test, $n = 178$ pairs) and from new mothers 1.0584 ± 0.009 ($p = 1.07 \times 10^{-8}$, two-tailed paired *t*-test, $n = 177$ pairs). The two ratios were significantly different from each other ($p = 0.03$, one-tailed non-paired *t*-test), showing a higher asymmetry between the daughters coming from old mothers than from new mother. New daughters in general had a higher elongation rate than old daughters with an average ratio of 1.07 ± 0.006 ($p = 1.96 \times 10^{-23}$, two-tailed paired *t*-test), consistent with the fluorescence ratios mentioned in figure 3*a,b*. (Online version in colour.)

the same cell lengths for comparison (figure 2*b*). Fluorescence along the cells was biased towards the new poles and not uniformly distributed.

To quantify the bias towards new poles, we compared the old and new pole difference between old and new daughters (figure 1). We found that the new pole was significantly brighter than the old pole in both new and old daughters ($p = 3.41 \times 10^{-48}$ and 2.58×10^{-97}, respectively) (figure 3*a*). However, the fluorescence ratio of new to old poles was 1.2 ± 0.06 (s.e.m.) in old daughters and 1.11 ± 0.006 in new daughters, and the pole ratio of old daughters was significantly larger than that of old daughters ($p = 2.8 \times 10^{-19}$). If the old and new poles were pooled to obtain the total fluorescence for single cells of new and old daughters, new daughters were significantly brighter ($p = 2.57 \times 10^{-65}$) and the daughter fluorescence ratio (new/old) was 1.08 ± 0.004.

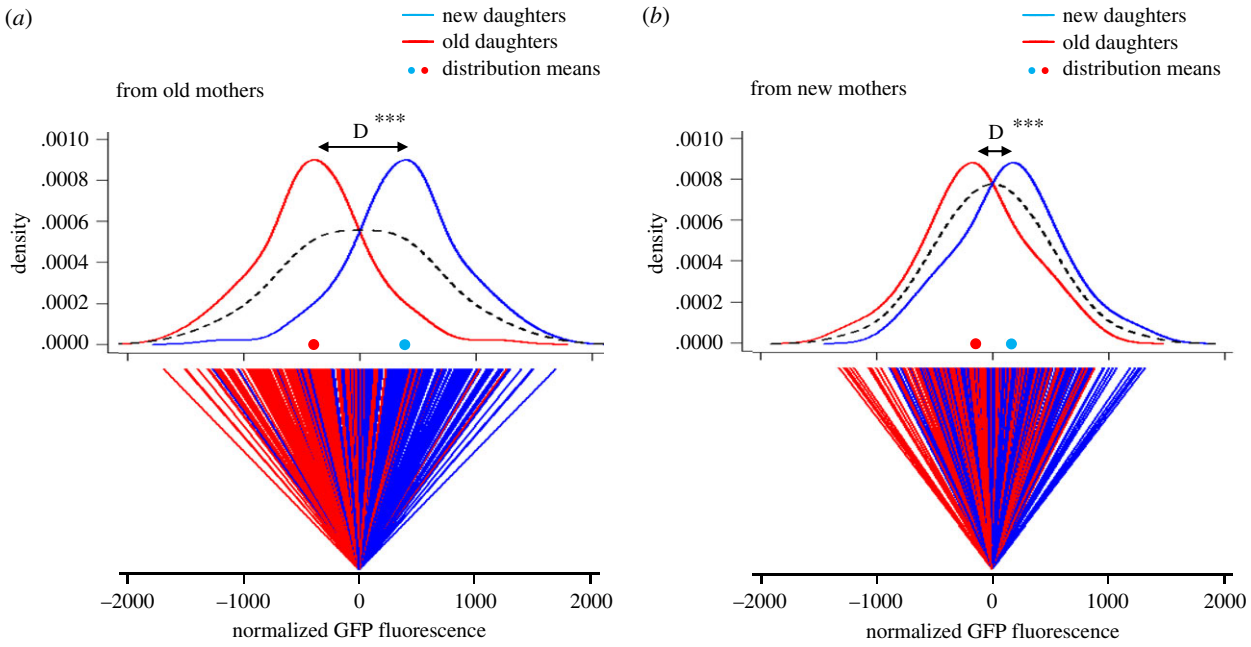

Figure 4. Deterministic variance of fluorescence between new and old daughters from old and new mothers. (*a*) Top panel: Normalized density—distribution—of fluorescence of new (blue) and old (red) daughters from old mothers ($n = 178$ daughter pairs). Dots on the *x*-axis indicate the average fluorescence for each distribution. 'D' (black arrow) stands for the distance between peaks of new and old daughter curves. Significance for 'D' as determined from ratios between new and old daughters in the legend to figure 3. The average population density, combining new and old daughters, is indicated by dashed lines. Bottom panel: Normalized fluorescence of each new (blue) and old (red) daughter pairs from old mothers. The zero point is the average fluorescence between each pair. As can be seen, the old daughter in each pair more often ends up on the minus side of the pair's zero point, i.e. having less fluorescence. The deterministic asymmetry when the daughters come from old mothers was calculated to constitute 40% of what normally is reported as stochasticity. (*b*) The same as (*a*), but from new mothers. $n = 177$ daughter pairs. The deterministic asymmetry when the daughters originate from new mothers (bottom panel) was calculated to constitute 10% of what normally is reported as stochasticity. (Online version in colour.)

(b) Deterministic asymmetry of green fluorescent protein fluorescence is higher in daughters from old mothers than from new mothers

Because pole fluorescence was more similar in new daughters than in old ones, we hypothesized that fluorescence between daughters from new mothers should be more similar than between daughters from old mothers. To identify old and new mothers, which were mothers born, respectively, as old or new daughters, we tracked the divisions for an additional generation beyond lineages presented in figure 1. As before (see above), the new daughters from both new and old mothers were brighter ($p = 1.78 \times 10^{-5}$ and $p = 1.68 \times 10^{-21}$, respectively). However, old mothers produced significantly ($p = 2.75 \times 10^{-9}$) more different daughters than new mothers, as demonstrated by the respective daughter fluorescence ratios of 1.12 ± 0.009 and 1.04 ± 0.008 (figure 3*b*). Note that the average of the 1.12 and 1.04 ratios replicates closely the value of 1.08 that was obtained for the pooled daughters in the above section.

(c) Deterministic asymmetry accounts for a large component of the variance of expressed gene products in a population

To determine how much of the variation of expressed gene products in single cells is explained by deterministic asymmetry, we estimated the total variance (V_T), the subcomponents attributable to deterministic asymmetry (V_A) and error or unexplained factors (V_E), and $V_T = V_A + V_E$. In the absence of more information, V_E can be interpreted to represent the stochastic component [15].

V_T, V_A and V_E were estimated separately for old and new mothers depicted in figure 3*a*. To obtain estimates for one mother type, the variance of fluorescence levels in its new and old daughters, V_{New} and V_{Old}, was first determined (figure 4). V_T was then estimated from a pool consisting of all the old and new daughters. If deterministic asymmetry is absent, V_{Old} and V_{New} are the sole components, $V_A = 0$, and $V_T = V_E = (V_{Old} + V_{New})/2$. If deterministic asymmetry renders the fluorescence level of new daughters higher, the difference $D = M_{New} - M_{Old} > 0$, where M_{New} and M_{Old} are the mean fluorescence levels of the new and old daughters. Because $D > 0$ pushes apart the old and new daughter distributions and inflates V_T (figure 4), $V_T = (V_{Old} + V_{New})/2 + D^2/4$ [19]. The deterministic component of variance V_A is the term $D^2/4$, in which case $V_A = V_T - (V_{Old} + V_{New})/2$. The contribution of deterministic asymmetry expressed as a percentage is

$$h^2 = V_A/V_T = 1 - (V_{Old} + V_{New})/2V_T = 1 - V_E/V_T$$

Our results showed that $h^2 = 10.1$ and 40.1% for new and old mothers (figure 4*a*,*b*). The higher h^2 for older mothers is consistent with our results that old poles have less fluorescence (figure 3*a*) and that old mothers have daughters that are more different (figure 3*b*). An old pole in an old mother is older than the old pole in a new mother and therefore has lesser fluorescence than the old pole in the new mother. In other words—the more different the poles, the more different the daughters. Thus, a substantial proportion of the variation of expressed gene products previously attributed to stochasticity in single *E. coli* cells results from the deterministic

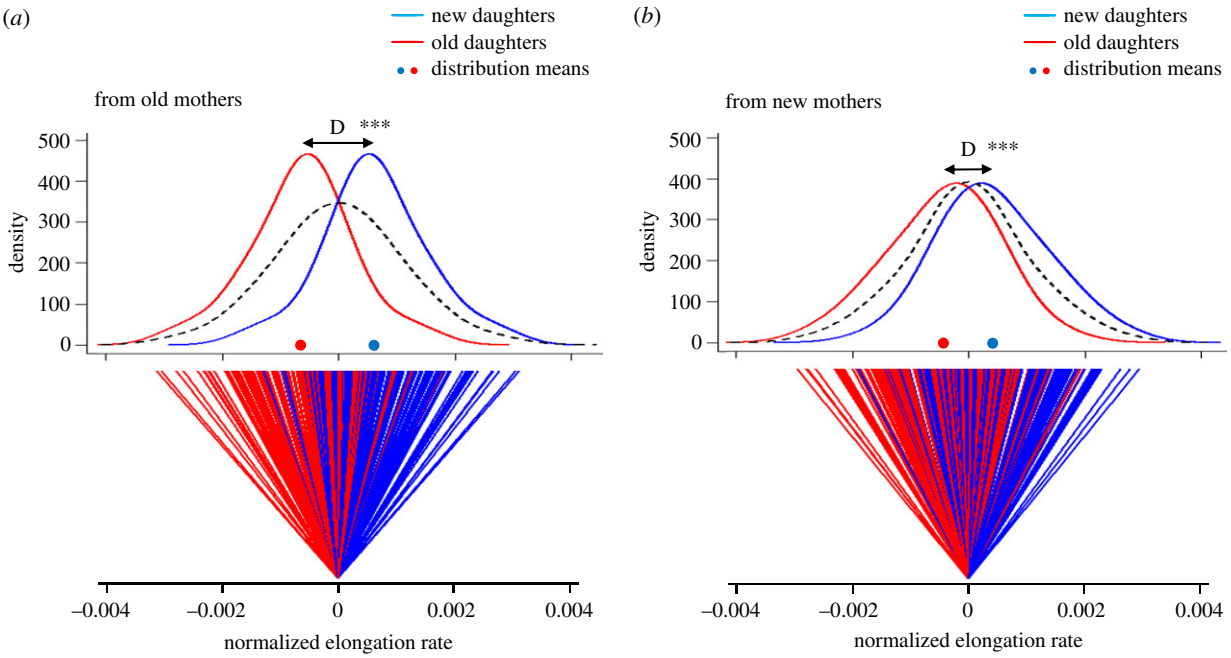

Figure 5. Deterministic variance of elongation rate between new and old daughters from old and new mothers. (*a*) Top panel: Density—distribution—of elongation rate of new (blue) and old (red) daughters from old mothers ($n = 178$ daughter pairs). Dots on the *x*-axis indicate the average fluorescence for each distribution. 'D' (black arrow) stands for the distance between peaks of new and old daughter curves. Significance for 'D' as determined from ratios between new and old daughters in the legend to figure 3. The average population elongation rate, combining new and old daughters, is indicated by dashed lines. Bottom panel: Normalized elongation rate of new (blue lines) and old (red lines) daughter pairs from old mothers. The zero point is the average elongation rate between each pair. As can be seen, the old daughter in each pair more often ends up on the minus side of the pair's zero point, i.e. having a slower elongation rate. The deterministic asymmetry when the daughters come from old mothers was calculated to constitute 32.2% of the total variance. (*b*) Same as as (*a*), but from new mothers. $n = 177$ daughter pairs. The deterministic asymmetry of daughters coming from new mothers was calculated to be 16.9% of the total variance. (Online version in colour.)

process by which more expressed gene products are allocated to new daughters. The amount $V_E = (V_{Old} + V_{New})/2$ that remains unexplained and attributed to stochasticity could be further reduced if other deterministic processes are uncovered.

(d) Deterministic component of variance for elongation rates of single cells

Because elongation rates in *E. coli* have a deterministic asymmetric component of variance [17,18], the cells quantified for fluorescence in figure 4 were further examined to determine whether they manifested a similar asymmetry and variance pattern for elongation rates and whether GFP and elongation rates were correlated. Elongation rates were measured (see Material and Methods) for all daughters and grouped by old and new mothers. The effect of deterministic asymmetry on elongation rates was clear. If the old and new mothers were pooled, the new daughters had a significantly higher elongation rate ($p = 1.96 \times 10^{-23}$), and the ratio of the rates was 1.07 ± 0.006 in favour of new daughters. Moreover, new daughters had a significantly higher rate than old daughters regardless of whether they came from an old or new mother ($p = 1.12 \times 10^{-16}$ and $p = 1.07 \times 10^{-8}$, respectively; ratios of 1.083 ± 0.009 and 1.059 ± 0.009) (figure 3*c*). The ratios of 1.0833 and 1.0584 were significantly different by a one-tail *t*-test ($p = 0.03$), and the higher ratio suggested again that difference between daughters was bigger in old mothers. Thus, we partitioned the variance of elongation rates to estimate the deterministic fraction. Using the same approach followed for fluorescence (cf. Figure 4), we estimated that the variance component due to deterministic asymmetry was $h^2 = 16.9$ and 32.2% for elongation rates of daughters from new and old mothers (figure 5). Thus, just as GFP fluorescence in single *E. coli* cells, elongation rates are highly stochastic but a large fraction is deterministic.

(e) Correlation between green fluorescent protein fluorescence and elongation rate of single cells

Because the patterns of fluorescence and elongation rate in old and new daughters and mothers were similar, we tested next whether the two traits could be related. A test for correlation revealed that fluorescence and elongation rates were positively correlated, however, only significant when coming from old mothers. Daughters from old mothers showed a strong and significant correlation ($r = 0.26$, $p = 0.0066$) (figure 6*a*), while daughters from new mothers exhibited a weaker and not significant association ($r = 0.041$, $p = 0.14$) (figure 6*b*). The correlations from old mothers were also significantly larger than the correlations from new mothers ($p = 0.012$). The correlation between elongation rate and fluorescence is consistent with early reports that show positive correlations between ribosome levels, which produce proteins, and growth rate [29,34]. It is also consistent with figures 4 and 5 that show that asymmetry between daughter cells is always higher when originating from old mothers, which allocate more of the damaged proteins to her old daughter [18] and more newly synthesized proteins to her new daughter.

3. Discussion

Our results show that expressed gene products, much like cell growth or elongation rates, have both a stochastic and a

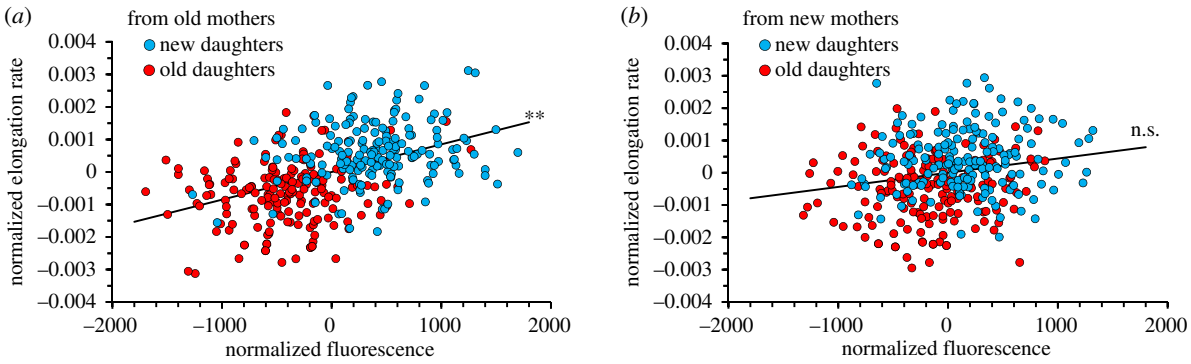

Figure 6. Correlation between normalized GFP fluorescence and normalized elongation rate showing a higher rate when daughters come from old mothers than from new mothers. Because the normalized values did not conform to a standard Gaussian distribution, the correlation statistics and comparisons were conducted by randomizing the data and obtaining a null distribution of correlations. The *p*-values reported represent the probability that the observed correlation is exceeded by the correlations of the null distribution. (*a*) Normalized fluorescence versus normalized elongation rate between new and old daughters from old mothers. Correlation $r = 0.24$, $p = 0.0066$ (**), $n = 178$ daughter pairs. (*b*). Normalized fluorescence versus normalized elongation rate between new and old daughters from new mothers. Correlation $r = 0.041$, $p = 0.14$ (n.s.), $n = 177$ daughter pairs. A comparison of observed correlation from old and new mothers (figure 6*a* versus b) was found to be significant ($p = 0.012$). (Online version in colour.)

deterministic component. The deterministic components are manifested in single cells as a consistently higher level of reported GFP fluorescence in the new poles relative to the old poles of a bacterium. If the data, originally reported as ratios (figure 3*a*), are re-expressed as per cent differences, new poles showed 5.2 and 9.1% more fluorescence in new and old daughters, respectively. The difference between the poles is unlikely explained by differential rates of localized gene expression. The mean length of the *E. coli* cells in this study was 3.6 µm and the mean doubling time was 40.2 min. The GFP mut3b variant used for our study has a maturation time of $t_{50} = 4$ min [30] and a diffusion rate of 9 $\mu m^2 s^{-1}$ [31]. With such a high diffusion rate, mature and fluorescent GFP molecules should effectively have a uniform distribution in the absence of any interfering factors. The presence of aggregates in the old poles of cells [25] suggests that an interfering factor could be limiting space. With more damage in the old pole, newly expressed gene products would find more space to occupy in the new pole. Because the maternal old pole is allocated to the old daughter (figure 1), space limitation due to the damage in the old pole is anticipated to restrict the abundance of expressed GFP in the old daughter. This prediction is supported by our observation that new daughters were always more fluorescent than old daughters, although the difference was greater when daughter pairs came from old mothers (2.0 and 5.7% difference; new versus old mothers; figure 3*b*). Our reported differences between new and old poles in new and old daughter (5.2 versus 9.1%) and between new and old daughters from new and old mothers (2.0 versus 5.7%) also demonstrate a consistency that supports a possible role for damage. The difference is smaller for new daughters and for new mothers because they have less damage to create the difference. This is further shown by our estimates of the deterministic variance component explained by asymmetry. Deterministic asymmetry accounts for 10.1% of the total variance of GFP fluorescence in daughter pairs of new mothers, but 40.1% in old mothers (figure 4*a*).

Because there is a strong correlation between elongation rate and the ribosome levels [29,34–36], it follows that the expressed level of gene products could also correlate with elongation rates. Our results confirmed this correlation between elongation rate and protein levels using GFP production as a proxy for expressed proteins and measuring elongation rate of the same cells (figure 6*a*,*b*). The strength of these correlations is noteworthy for two reasons. First, because the production of GFP can be costly to cell growth [37], the correlation shows that it can, at the levels observed in our study, serve as a proxy for expressed gene products. The correlation may in fact be stronger because it may have been attenuated by the cost. Second, the stronger correlation in daughters produced by old mothers (figure 6*a*) supports again our suggestion that GFP levels, and now growth rates, could result from the space limitation. Because old mothers have more damage, their old and new daughters have more divergent levels of damage, gene products and growth rates. New daughters, compared to old daughters, had 2.9 versus 4.0% higher elongation rates when produced, respectively, by new and old mothers (figure 3*c*). Space limitation is additionally supported by similarity between the effects of deterministic asymmetry on variation in expressed GFP levels and elongation rates. Deterministic asymmetry accounted for 32.2 versus 16.9% of total variance when old and new daughter pairs were produced by old versus new mothers (figure 5*a*,*b*). Thus, our results show that the amount of expressed gene products and elongation rates in single cells are highly variable, but cannot be entirely attributed to stochasticity. When the age of a mother cell is considered, deterministic components account for a large fraction of single-cell variability.

A tempting hypothesis at this juncture is that the space occupied by aggregates limits the amount of ribosomes in a cell and therefore reduces the level of expressed proteins and the final elongation rate. We recognize that the observed relationships we use to formulate this hypothesis could be correlational and not causal. The hypothesis is only meant for stimulating discussion and future testing. However, because it has been shown that the addition of an external damage agent to cells decreases elongation rates [18], damage may be the trigger that starts the process. Because aggregates of damaged proteins tend to accumulate more in old poles and old daughters [25], and less in new poles and new daughters, the resulting asymmetry has a marked effect on the bacterial population [17,24]. Lineages of old daughters accumulate increasingly more damage and the new daughters decreasingly less damage. While the old daughter lineage

grows more slowly and ages, the new daughter lineage grows more rapidly and rejuvenates. However, because the total damage a cell has at birth is diluted by growth and increasing cell size, the accumulation of damage in the old daughter lineage increases only until the point at which the rate of increase is cancelled by the dilution. At this point, the growth rate of the old daughters stabilizes at an equilibrium value. Likewise, an equilibrium is achieved by the new daughter's lineage. However, because new daughters are allocated less damage, the equilibrium growth rate for those cells is higher than for old daughters. Thus, old daughters that are grown under standard laboratory conditions age but only until the equilibria. There is no death and the lineages are immortal. However, if the damage rate is increased by introducing external damage agents, such as phototoxicity, antibiotics or heat, the old daughter equilibrium can be destabilized and the lineage dies. With the death, aging makes the lineage mortal.

The asymmetry between the growth rate of old and new daughters (figures 3*c*, 5*a*,*b*) is in principle evolutionarily advantageous to the bacteria. The growth rate difference between the old and new daughters creates fitness variation that increases the efficiency of natural selection for eliminating the damage from the population. A more intuitive explanation comes from a banking analogy comparing one account started with \$1,000 and an interest rate of 8% yr^{-1} and two accounts with \$500 at 6% and \$500 at 10%. Splitting the \$1,000 into the two \$500 accounts yields more returns after 1 year because of the 10% returns. A bacterial lineage that allocates damage asymmetrically to its daughters likewise gains higher growth rate or fitness returns from the new daughters. The analogy is not perfect because bacterial lineages split the damage every generation. However, in both cases, the outcomes are predicted by Jensen's Inequality [38]. If the returns are generated by a greater than linear process, such as exponential population growth or interest rates, they are increased by increasing the variance of the initial states.

Cell growth rate variance created by random stochasticity alone can generate the advantage provided by Jensen's Inequality [19]. Lineages that by chance received more damage would also age, attain stable equilibrium states and become mortal with high rates of damage. However, although these lineages, along with their aging and rejuvenation, could be readily tracked by time-lapse microscopy, they would show no association with old poles and old daughters. Damage could accumulate equally in either old or new poles or daughters. The fact that damage aggregates and aging are associated with old poles and daughters in *E. coli* [17,18,20,21,25,39–42] has led us to suggest that the partitioning may have been polarized by anchored, and thus not diffusible or movable, damage [19]. By virtue of being older, old poles most likely harboured the initial anchored damage. Allocating damage to the new pole would have countered the damage anchored to the old pole and the variance between old and new daughters would have been decreased. On the other hand, the variance is increased by polarizing the allocation to the old pole. Because aggregates in *E. coli* are sticky [39], an aggregate at the old pole grows as other aggregates adhere to it. Whether aggregate stickiness is an inherent property of damaged proteins, or a trait evolved to concentrate damage to the old pole, is debatable and not known. Regardless, the asymmetric distribution of damage, and now also of expressed gene products (figures 2*a*,*b*, 3*a*,*b*, 4*a*,*b*), is a deterministic process that increases the variance of single cells in an *E. coli* population.

4. Material and methods

(a) Bacterial strains, growth media and green fluorescent protein reporter

Growth experiments were performed using *E. coli* K12 (NCM3722 *ΔmotA:frt*, *chromosomal:T:ptet-GFP:frt*) [43], which has a chromosomal insert of constitutively expressed native *gfp*, unfused to any protein and thereby with no deterministic spatial placement in the cell as a mature protein. Cells were grown in M9 minimal media [44] supplemented with 0.02 mg ml^{-1} of thiamine and 0.18 mg ml^{-1} of glucose as the carbon source. Protein levels were quantified by using GFP as a reporter. Because native GFP is estimated to have a diffusion rate of 9 $\mu m^2 s^{-1}$ [31] and the *E. coli* cell has a mean cross-sectional area of about 3 μm^2, the protein is rapidly dispersed throughout a cell in less than 1 s. Because our fluorescence images were taken at 20 min intervals, the distribution of GFP densities in a mother cell, and consequently also in the daughters, is not diffusion limited. Rather, the different densities result from differential production or gene expression within the cells. The strain was kindly provided by Minsu Kim (Emory University).

(b) Cell growth and microscope slides

Cells from −80°C glycerol stock were streaked onto agar plates. A single colony was inoculated into M9 media and grown at 37°C overnight. The following day the culture was diluted 1:100 in M9 and grown for 2 h. One microlitre of the culture was then pipetted onto a 10 µl M9 agarose pad. The agarose pad was then was then flipped with the bacterial side down onto a 24 × 60 mm cover glass and placed over a 25 × 75 mm single depression slide sealed with vaseline (modified from earlier methods described in [20,21,23] to fit an inverted microscope). Individual cells from two different movies were followed through time-lapse microscopy at 37°C until each grew into a micro-colony of 64 cells.

(c) Time-lapse microscopy

Cells were imaged with an inverted microscope (Nikon Eclipse Ti-S), equipped with Nikon NIS-Elements AR control software, 100X objective (CFI Plan APO NA 1.4), external phase contrast rings for full intensity fluorescence imaging (FITC), fluorescence light source (Prior Lumen 200) with motorized shutter (Lambda 10-B Sutter SmartShutter) and camera (Retiga 2000R FAST 1394, mono, 12 bit). Phase contrast and fluorescence images were recorded every 2 and 20 min, respectively.

(d) Image quantification and analysis

Fluorescence measurements were collected by tracing cell outlines on the phase contrast images, transferring the outlines to the corresponding fluorescence frame and quantifying density of fluorescence inside the outline. Outlines were traced manually. Blind replicate outlines, made without any awareness of cell polarity, reproduced the same results. All fluorescence images were corrected by removing outliers, subtracting background and deconvoluted to correct for diffraction scattering. The software ImageJ (NIH) was used for quantifying fluorescence densities, outlier removal and background subtraction. Fluorescence measurements were collected by first tracing cell outlines on the phase contrast images, and the corresponding fluorescent frame was processed as following: the background of each frame was subtracted using 'rolling ball' algorithm in ImageJ with ball radius 20 pixels. Noise created by heat overflow of single pixel was corrected by 'remove outliers' algorithm in ImageJ with threshold intensity difference 1000 and threshold radius 0.5 pixel. Deconvolution was accomplished by the Lucy-Richardson method in Matlab 2017b (The MathWorks, Inc., Natick, MA),

(see electronic supplementary material for details). Fluorescence measurements for pairs of old and new daughters were normalized by subtracting the mean of the pair's values. To calculate elongation rates, lengths of individual bacterial cells were extracted manually from recorded time-lapse images with ImageJ. From lengths compiled over time, the elongation rate r was estimated as the slope of a linear regression of (log/length) over time. A log transformation was used because elongation rates are known to be exponential [20]. All lengths were measured immediately after division and prior the next division.

(e) Statistical tests

All comparisons were evaluated by either *t*-tests or randomized designs. Details of sample sizes and choices of paired, unpaired, one- and two-tailed comparisons are provided in the figure legends. Randomized designs were used when data did not conform to standard Gaussian requirements. When appropriate, values are presented as mean ± s.e.m. (standard error of the mean).

Data accessibility. Data are available from the Dryad Digital Repository: https://doi.org/10.6075//dryad.J0542M0K [45].

Authors' contributions. C.U.R. conceived the study. C.U.R., L.C. and C.S. designed and conducted the experiments. C.U.R., A.M.P. and C.S. collected the data. J.U.C. and A.Q. conducted blind controls. L.C., C.U.R. and C.S. analysed the results. L.C. and C.S. developed the deconvolution analysis. C.S., L.C. and C.U.R. wrote the manuscript.

Competing interests. We declare we have no competing interests.

Funding. Work was supported by grants to L.C. from the National Science Foundation (DEB-1354253) and funds from Donald Helinski. A.M.P. was supported by the Science Without Borders Fellowship/CAPES—Brazil.

Acknowledgements. We thank Kevin Chi and Xiyu Liu for assistance.

References

1. Thattai M, van Oudenaarden A. 2001 Intrinsic noise in gene regulatory networks. *Proc. Natl Acad. Sci. USA* **98**, 8614–8619. (doi:10.1073/pnas.151588598)
2. Elowitz MB, Levine AJ, Siggia ED, Swain PS. 2002 Stochastic gene expression in a single Cell. *Science* **297**, 1183–1186. (doi:10.1126/science.1070919)
3. Raser JM, O'Shea EK. 2005 Noise in gene expression: origins, consequences, and control. *Science* **309**, 2010–2013. (doi:10.1126/science.1105891)
4. Rosenfeld N, Young JW, Alon U, Swain PS, Elowitz MB. 2005 Gene regulation at the single-cell level. *Science* **307**, 1962–1965. (doi:10.1126/science.1106914)
5. Wang Z, Zhang J. 2011 Impact of gene expression noise on organismal fitness and the efficacy of natural selection. *Proc. Natl Acad. Sci. USA* **108**, E67–E76. (doi:10.1073/pnas.1100059108)
6. Kiviet DJ, Nghe P, Walker N, Boulineau S, Sunderlikova V, Tans SJ. 2014 Stochasticity of metabolism and growth at the single-cell level. *Nature* **514**, 376–379. (doi:10.1038/nature13582)
7. Kærn M, Elston TC, Blake WJ, Collins JJ. 2005 Stochasticity in gene expression: from theories to phenotypes. *Nat. Rev. Genet.* **6**, 451–464. (doi:10.1038/nrg1615)
8. Raj A, van Oudenaarden A. 2008 Nature, nurture, or chance: stochastic gene expression and its consequences. *Cell* **135**, 216–226. (doi:10.1016/j.cell.2008.09.050)
9. Sanchez A, Choubey S, Kondev J. 2013 Regulation of noise in gene expression. *Ann. Rev. Biophys.* **42**, 469–491. (doi:10.1146/annurev-biophys-083012-130401)
10. Huh D, Paulsson J. 2011 Random partitioning of molecules at cell division. *Proc. Natl Acad. Sci. USA* **36**, 15 004–15 009. (doi:10.1073/pnas.1013171108)
11. Guptasarma P. 1995 Does replication-induced transcription regulate synthesis of the myriad low copy number proteins of *Escherichia coli*? *Bioessays* **17**, 987–997. (doi:10.1002/bies.950171112)
12. Carey JN, Mettert EL, Roggiani M, Myers KS, Kiley PJ, Goulian M. 2018 Regulated stochasticity in a bacterial signaling network permits tolerance to a rapid environmental change. *Cell* **173**, 196–207. (doi:10.1016/j.cell.2018.02.005)
13. Veening JW, Stewart EJ, Berngruber TW, Taddei F, Kuipers OP, Hamoen LW. 2008 Bet-hedging and epigenetic inheritance in bacterial cell development. *Proc. Natl Acad. Sci. USA* **105**, 4393–4398. (doi:10.1073/pnas.0700463105)
14. Huang S. 2009 Non-genetic heterogeneity of cells in development: more than just noise. *Development* **136**, 3853–3862. (doi:10.1242/dev.035139)
15. Zernicka-Goetz M, Huang S. 2010 Stochasticity versus determinism in development: a false dichotomy? *Nat. Rev. Genet.* **11**, 743–744. (doi:10.1038/nrg2886)
16. Bergmiller T, Andersson AMC, Tomasek K, Balleza E, Kiviet DJ, Hauschild R, Tkačik G, Guet CC. 2017 Biased partitioning of the multidrug efflux pump AcrAB-TolC underlies long-lived phenotypic heterogeneity. *Science* **356**, 311–315. (doi:10.1126/science.aaf4762)
17. Proenca AM, Rang CU, Buetz C, Shi C, Chao L. 2018 Age structure landscapes emerge from the equilibrium between aging and rejuvenation in bacterial populations. *Nat. Commun.* **9**, 1–11. (doi:10.1038/s41467-018-06154-9)
18. Proenca AM, Rang CU, Qiu A, Shi C, Chao L. 2019 Cell aging preserves cellular immortality in the presence of lethal levels of damage. *PLoS Biol.* **17**, e3000266. (doi:10.1371/journal.pbio.3000266)
19. Chao L, Rang CU, Proenca AM, Chao JU. 2016 Asymmetrical damage partitioning in bacteria: a model for the evolution of stochasticity, determinism, and genetic assimilation. *PLoS Comput. Biol.* **12**, 1–17. (doi:10.1371/journal.pcbi.1004700)
20. Stewart EJ, Madden R, Paul G, Taddei F, Burland V. 2005 Aging and death in an organism that reproduces by morphologically symmetric division. *PLoS Biol.* **3**, e45. (doi:10.1371/journal.pbio.0030045)
21. Rang CU, Peng AY, Chao L. 2011 Temporal dynamics of bacterial aging and rejuvenation. *Curr. Biol.* **21**, 1813–1816. (doi:10.1016/j.cub.2011.09.018)
22. Rang CU, Proenca A, Buetz C, Shi C, Chao L. 2018 Minicells as a damage disposal mechanism in *Escherichia coli*. *mSphere* **3**, e00428-18. (doi:10.1128/mSphere.00428-18)
23. Rang CU, Peng AY, Poon AF, Chao L. 2012 Ageing in *Escherichia coli* requires damage by an extrinsic agent. *Microbiol.* **158**, 1553–1559. (doi:10.1099/mic.0.057240-0)
24. Chao L. 2010 A model for damage load and its implications for the evolution of bacterial aging. *PLoS Genet.* **6**, e1001076. (doi:10.1371/journal.pgen.1001076)
25. Lindner AB, Madden R, Demarez A, Stewart EJ, Taddei F. 2008 Asymmetric segregation of protein aggregates is associated with cellular aging and rejuvenation. *Proc. Natl Acad. Sci. USA* **105**, 3076–3081. (doi:10.1073/pnas.0708931105)
26. Urszula Ł, Glover G, Capilla-lasheras P, Young AJ, Pagliara S, Young AJ, Pagliara S. 2019 Bacterial ageing in the absence of external stressors. *Phil. Trans. R. Soc. B* **374**, 20180442. (doi:10.1098/rstb.2018.0442)
27. Govers SK, Mortier J, Adam A, Aertsen A. 2018 Protein aggregates encode epigenetic memory of stressful encounters in individual *Escherichia coli* cells. *PLoS Biol.* **16**, e2003853. (doi:10.1371/journal.pbio.2003853)
28. Lele UN, Baig UI, Watve MG. 2011 Phenotypic plasticity and effects of selection on cell division symmetry in *Escherichia coli*. *PLoS ONE* **6**, e14516. (doi:10.1371/journal.pone.0014516)
29. Schaechter M, Maaløe O, Kjeldgaard NO. 1958 Dependency on medium and temperature of cell size and chemical composition during balanced growth of *Salmonella typhimurium*. *J. Gen. Microbiol.* **19**, 592–606. (doi:10.1099/00221287-19-3-592)
30. Balleza E, Kim JM, Cluzel P. 2018 Systematic characterization of maturation time of fluorescent proteins in living cells. *Nat. Methods.* **15**, 47–51. (doi:10.1038/nmeth.4509)

31. Mullineaux CW, Nenninger A, Ray N, Robinson C. 2006 Diffusion of green fluorescent protein in three cell environments in *Escherichia coli*. *J. Bacteriol.* **188**, 3442–3448. (doi:10.1128/JB.188.10.3442-3448.2006)
32. Cormack BP, Valdivia RH, Falkow S. 1996 FACS-optimized mutants of the green fluorescent protein (GFP). In *Gene*, pp. 33–38. Amsterdam, The Netherlands: Elsevier B.V. (doi:10.1016/0378-1119(95)00685-0)
33. Sundararaj S. 2004 The CyberCell Database (CCDB): a comprehensive, self-updating, relational database to coordinate and facilitate *in silico* modeling of *Escherichia coli*. *Nucleic Acids Res.* **32**, 293–295. (doi:10.1093/nar/gkh108)
34. Kjeldgaard NO, Kurland CG. 1963 The distribution of soluble and ribosomal RNA as a function of growth rate. *J. Mol. Biol.* **6**, 341–348. (doi:10.1016/S0022-2836(63)80093-5)
35. Poulsen LK, Licht TR, Rang C, Krogfelt KA, Molin S. 1995 Physiological state of *Escherichia coli* BJ4 growing in the large intestines of streptomycin-treated Mice. *J. Bacteriol.* **177**, 5840–5845. (doi:10.1128/JB.177.20.5840-5845.1995)
36. Rang CU, Licht TR, Midtvedt T, Conway PL, Chao L, Krogfelt KA, Cohen PS, Molin S. 1999 Estimation of growth rates of *Escherichia coli* BJ4 in streptomycin-treated and previously germfree mice by *in situ* rRNA hybridization. *Clin. Diagn. Lab. Immunol.* **6**, 434–436. (doi:10.1128/CDLI.6.3.434-436.1999)
37. Rang C, Galen JE, Kaper JB, Chao L. 2003 Fitness cost of the green fluorescent protein in gastrointestinal bacteria. *Can. J. Microbiol.* **49**, 531–537. (doi:10.1139/w03-072)
38. Perlman MD. 1974 Jensen's inequality for a convex vector-valued function on an infinite-dimensional space. *J Multivar Anal.* **4**, 52–65. (doi:10.1016/0047-259X(74)90005-0)
39. Coquel A-SS, Jacob J-PP, Primet M, Demarez A, Dimiccoli M, Julou T, Moisan L, Linder AB, Berry H. 2013 Localization of protein aggregation in *Escherichia coli* is governed by diffusion and nucleoid macromolecular crowding effect. *PLoS Comput. Biol.* 9, e1003038. (doi:10.1371/journal.pcbi.1003038)
40. Mortier J, Tadesse W, Govers SK, Aertsen A. 2019 Stress-induced protein aggregates shape population heterogeneity in bacteria. *Curr. Genet.* **65**, 11–16. (doi:10.1007/s00294-019-00947-1)
41. Tyedmers J, Mogk A, Bukau B. 2010 Cellular strategies for controlling protein aggregation. *Nat. Rev. Mol. Cell Biol.* **11**, 777–788. (doi:10.1038/nrm2993)
42. Winkler J *et al*. 2010 Quantitative and spatio-temporal features of protein aggregation in *Escherichia coli* and consequences on protein quality control and cellular ageing. *EMBO J.* **29**, 910–923. (doi:10.1038/emboj.2009.412)
43. Kim M, Zhang Z, Okano H, Yan D, Groisman A, Hwa T. 2012 Need-based activation of ammonium uptake in *Escherichia coli*. *Mol. Syst. Biol.* **8**, 616. (doi:10.1038/msb.2012.46)
44. Miller JH. 1972 *Experiments in molecular genetics*. Cold Spring Harbor, NY: Cold Spring Harbor Laboratory Press.
45. Shi C, Chao L, Proenca AM, Qiu A, Chao J, Rang CU. 2020 Data from: Allocation of gene products to daughter cells is determined by the age of the mother in single *Escherichia coli* cells. Dryad Digital Repository. (https://doi.org/10.6075//dryad.J0542M0K)